Acta Pharmaceutica Sinica B 2021;11(11):3542–3552

Chinese Pharmaceutical Association
Institute of Materia Medica, Chinese Academy of Medical Sciences

Acta Pharmaceutica Sinica B

www.elsevier.com/locate/apsb
www.sciencedirect.com

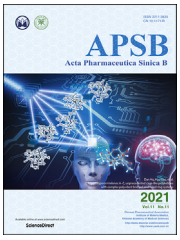

ORIGINAL ARTICLE

Discovery of a potent FKBP38 agonist that ameliorates HFD-induced hyperlipidemia *via* mTOR/P70S6K/SREBPs pathway

Ping-Ting Xiao[a,†], Zhi-Shen Xie[b,†], Yu-Jia Kuang[a], Shi-Yu Liu[a], Chun Zeng[c,*], Ping Li[a,*], E-Hu Liu[a,*]

[a]*State Key Laboratory of Natural Medicines, China Pharmaceutical University, Nanjing 210009, China*
[b]*Academy of Chinese Medical Sciences, Henan University of Chinese Medicine, Zhengzhou 450046, China*
[c]*Departments of Pediatrics and Cellular & Molecular Medicine, Pediatric Diabetes Research Center and Institute for Genomic Medicine, University of California, San Diego, La Jolla, CA 92093, USA*

Received 21 December 2020; received in revised form 29 January 2021; accepted 10 February 2021

KEY WORDS

FKBP38;
Hyperlipidemia;
3,5,6,7,8,3′,4′-heptamethoxyflavone;
mTOR;
SREBP

Abstract The mammalian target of rapamycin (mTOR)-sterol regulatory element-binding proteins (SREBPs) signaling promotes lipogenesis. However, mTOR inhibitors also displayed a significant side effect of hyperlipidemia. Thus, it is essential to develop mTOR-specific inhibitors to inhibit lipogenesis. Here, we screened the endogenous inhibitors of mTOR, and identified that FKBP38 as a vital regulator of lipid metabolism. FKBP38 decreased the lipid content *in vitro* and *in vivo via* suppression of the mTOR/P70S6K/SREBPs pathway. 3,5,6,7,8,3′,4′-Heptamethoxyflavone (HMF), a citrus flavonoid, was found to target FKBP38 to suppress the mTOR/P70S6K/SREBPs pathway, reduce lipid level, and potently ameliorate hyperlipidemia and insulin resistance in high fat diet (HFD)-fed mice. Our findings suggest that pharmacological intervention by targeting FKBP38 to suppress mTOR/P70S6K/SREBPs pathway is a potential therapeutic strategy for hyperlipidemia, and HMF could be a leading compound for development of anti-hyperlipidemia drugs.

*Corresponding authors. Tel./fax: +86 25 83271379.
E-mail addresses: liuehu2011@163.com (E-Hu Liu), liping2004@126.com (Ping Li), tzengchun@gmail.com (Chun Zeng).
†These authors made equal contributions to this work.
Peer review under responsibility of Chinese Pharmaceutical Association and Institute of Materia Medica, Chinese Academy of Medical Sciences.

https://doi.org/10.1016/j.apsb.2021.03.031

1. Introduction

Hyperlipidemia is a common metabolic disorder characterized by an increase of plasma lipids and/or lipoproteins, and is a key risk factor for obesity, atherosclerosis, and type II diabetes[1]. Currently, anti-hyperlipidemic drugs mainly function as lanosterol synthase inhibitors, squalene epoxidase inhibitors, diacyl glycerol acyl transferase inhibitors, and ATP citrate lyase inhibitors. However, these anti-hyperlipidemic agents including statins and fibrates, are reported to have severe side effects on the muscles and liver[2]. It is not known whether other novel targets can be identified as anti-hyperlipidemic therapeutic agents.

In mammals, the biosynthesis of cholesterol, fatty acid (FA), and triglyceride (TG) are tightly regulated by sterol regulatory element-binding proteins (SREBPs) through activating the expression of rate-limiting lipogenic and cholesterogenic genes[3]. SREBPs activity is enhanced by the mammalian target of rapamycin (mTOR) to promote hepatic lipogenesis[4–6]. However, a significant side effect of hyperlipidemia has been observed in rodents and humans treated with mTOR inhibitor rapamycin[7,8]. Hence, there is an urgent need to develop mTOR-specific inhibitors which also can inhibit lipogenesis.

FKBP prolyl isomerase 38 (FKBP38, also known as FKBP8), an endogenous mTOR inhibitor[9], is a member of FK506 binding proteins (FKBPs) which elicit their function through direct binding and altering conformation of their target proteins, hence acting as molecular switches[10]. Here, we found that FKBP38 plays a vital role in the regulation of mTOR/P70S6K/SREBPs pathway and lipid homeostasis. Knockdown of *FKBP38* resulted in enhanced SREBP processing and lipid level both *in vitro* and *in vivo*. Importantly, we identified a natural flavonoid, 3,5,6,7,8,3′,4′-heptamethoxyflavone (HMF), binds to FKBP38 using docking approach, and demonstrated that HMF can activate FKBP38 to suppress mTOR/P70S6K/SREBPs pathway, reduce lipid level, and potently ameliorate hyperlipidemia in high fat diet (HFD)-fed mice.

2. Materials and methods

2.1. Animals

We obtained 6-week-old male C57BL/6J mice from Sino-British SIPPR/BK Lab Animal Ltd. (Shanghai, China), and kept them under a 12-h light/dark circle. For the HFD experiments, mice were fed with either normal diet (13.5% of energy from fat, normal diet, Nanjing Qinglong Mountain Laboratory Animal Co., Ltd., Nanjing, China) or HFD (normal chow supplemented with 1.25% cholesterol, 20% fat, and 0.5% cholic acid, *w*/*w*) for 6 weeks. For HMF experiments, mice were once daily oral gavage with vehicle, 25 or 50 mg/kg HMF (Weikeqi, China), or 30 mg/kg lovastatin (LOV, Aladdin, China) for 42 days.

The procedures for experiments and animal care were approved by the Institutional Animal Care and Use Committee of China Pharmaceutical University (Nanjing, China). Animal testing and research conforms to all relevant ethical regulations. All institutional and national guidelines for the care and use of laboratory animals were followed.

2.2. Cell lines

HL7702 and HepG2 (ATCC, USA) were grown in DMEM (Corning, USA) supplemented with 100 U/mL penicillin, 100 μg/mL streptomycin, and 10% (*v*/*v*) fetal bovine serum (FBS, Gibco, USA) at 37 °C in a 5% CO_2 incubator.

2.3. Cell viability assay

After seeded for 18 h, the HL7702 cells were administrated with HMF at the concentrations of 5, 10, 20, 40, and 80 μmol/L, respectively, for 18 h. 3-(4,5-Dimethylthiazol-2-yl)-2,5-diphenyltetrazoliumbromide (MTT) was added for 4 h, and detected the absorbance at 490 nm[11].

2.4. Nile-red staining

Cells were fixed with 4% paraformaldehyde (PFA) for 30 min, stained with 0.5 μg/mL nile-red (Macklin, China) after wash for 30 min at room temperature. Images were captured with fluorescence microscopy (Nikon, Japan), and quantified by Image Pro Plus 6.0 (Media Cybernetics, USA).

2.5. BODIPY (493/503) staining

Cells were fixed with 4% PFA for 30 min, stained with molecular probe 4,4-difluoro-1,3,5,7,8-pentamethyl-4-bora-3a,4a-diaza-*s*-indaceno (BODIPY 493/503, Invitrogen, USA) after wash at a concentration of 1 μg/mL at 37 °C for 15 min. Images were captured with fluorescence microscopy, and quantified by Image Pro Plus 6.0[12].

2.6. Luciferase assays

Cells were plated in 96-well plates at a density of 2.5×10^4 cells/well. After 18 h culture, cells were treated with or without 5, 10, or 20 μmol/L HMF with lipid depletion (LD) medium contained a 1:1 mixture of Ham's F-12 medium (GIBCO, USA) and DMEM supplemented with 100 U/mL penicillin, 100 μg/mL streptomycin sulfate, 5% lipoprotein-deficient serum (Kalen Biomedical, USA), 10 μmol/L compactin (Aladdin), and 50 μmol/L sodium mevalonate (Sigma, USA) for another 18 h. The luciferase activity was measured using luciferase assay kit (Promega, USA) and normalized by the concentration of total proteins using Enhanced BCA Protein Assay Reagent (Beyotime, China).

2.7. RNAs extraction, cDNA synthesis, and quantitative real-time reverse transcription PCR (qRT-PCR)

Total RNAs[13] were extracted using TRIzol (Vazyme, China) and cDNA synthesis was carried out using high capacity cDNA reverse transcription kit (Vazyme) according to the manufacturer's instructions. Gene expressions were measured by the Roche LightCycler 96 System (Roche, Switzerland) using SYBR-green. The mRNA expressions of respective genes were normalized to the mRNA levels of *Gadph* (mice) and *GAPDH* (human), or β-actin, and quantified by the $2^{-\Delta\Delta Ct}$ method. Primer sequences were described in Supporting Information Table S1.

2.8. Immunobloting

Cells and mouse liver were lysed in RIPA buffer supplemented with a protease inhibitor cocktail. Protein extracts were separated on 8%−10% SDS-PAGE gels and transferred onto nitrocellulose membranes. Then, the membranes were blocked in 5% non-fat milk for 1 h at room temperature. Protein expression was visualized by incubating primary antibodies overnight at 4 °C

followed by the corresponding secondary antibodies. Then, signals were detected with Tanon-5200 Chemiluminescent Imaging System (Tanon, Shanghai, China). The following antibodies were used: mTOR (#2983s), p-mTOR (Ser2448, #2971s), P70S6K (#9202s), p-P70S6K (Thr389, #9206s), AKT (#9272s), p-AKT (Ser473, #T4060s), p-GSK-3β (Ser9, #9323s), GSK-3β (#5558), p-AMPKα (Thr172, #2535s), and AMPKα (#5832s) (Cell Signaling Technology, USA); SREBP-2 (#ab30682, Abcam, USA); SREBP-1 (#sc-8984) and β-actin (#sc-81178) (Santa Cruz Biotechnology, USA); p-4EBP-1 (T36/47, #AP0030), 4EBP-1 (#A19045), and FKBP38 (#A7085) (Abclonal, China); anti-rabbit or mouse secondary antibodies (ZSGB-BIO, Beijing, China).

2.9. Immunohistochemistry

Paraffin-embedded tissue sections of mice livers were deparaffinized and rehydrated, followed by antigen retrieval using citrate buffer, and then permeabilized in 0.2% Triton X-100. Slides were blocked with 5% bovine serum albumin (BSA, Sigma) and treated with p-mTOR (Ser2448, #2976s, Cell Signaling Technology), p-P70S6K (Thr389, #AP0564, Abclonal, China), nucleus SREBP (n-SREBP)-1 (#sc-8984, Santa Cruz Biotechnology), and n-SREBP-2 (#ab30682, Abcam) followed by anti-mouse/rabbit polymer secondary antibodies and 3,3′-diaminobenzide tetrahydrochloride. Images were captured with digital pathological section scanner (NanoZoomer 2.0 RS, Hamamatsu, Japan).

2.10. Modeling docking

The X-ray crystal structure of FKBP38 [Protein Data Bank (PDB) code 2F2D], FKBP12 (PDB code 2PPN), FKBP4 (PDB code 4LAY), and FKBP51 (PDB code 6SAF) were used for the docking studies. Auto-dock 4.2 and PyRx 0.5 programs (The Scripps Research Institute, La Jolla, CA, USA) were employed for virtual screening, and the docked models were analyzed using Pymol 2.3 (DeLano Scientific LLC, San Carlos, CA, USA).

2.11. In vitro transfection

Cells were transfected with small interfering (siRNA) or plasmid using Lipofectamine® 2000 (Thermo Fisher Scientific, USA), and the gene expression level was measured 24 h after transfection. The siRNA oligo sequences are as follows: negative control (NC) siRNA: 5′-UUCUCCGAACGUGUCACGUTT-3′, 3′-ACGUGACACGUUCGGAGAATT-5′; *FKBP4* siRNA: 5′-GCUGGAACAGAGCACCAUATT-3′, 3′-UAUGGUGCUCUGUUCCAGCTT-5′; *FKBP10* siRNA: 5′-GCGGCACUUAUGACACCUATT-3′, 3′-UAGGUGUCAUAAGUGCCGCTT-5′; *FKBP12* siRNA: 5′-CCCUUUAAGUUUAUGCUAGTT-3′, 3′-CUAGCAUAAACUUAAAGGGTT-5′; *FKBP38* siRNA: 5′-CUGCAGUUGAAGGUGAAGUTT-3′, 3′-ACUUCACCUUCAACUGCAGTT-5′; *FKBP51* siRNA: 5′-GGGAGAAGAUCUGACGGAATT-3′, 3′-UUCCGUCAGAUCUUCUCCCTT-5′.

2.12. Ultrafiltration-liquid chromatography/mass spectrometry (LC/MS) analysis

For ultrafiltration, HMF (50 μmol/L) was incubated with 50 μg/mL Recombinant human FKBP38 proteins (ImmunoClone, USA) in the phosphate buffered saline (PBS) buffer at room temperature for 1 h. The control was prepared by using the binding buffer substitute for PBS during incubation. After incubation, each sample was filtered through a 10 kDa molecular weight cut-off ultrafiltration membrane by centrifugation. Then, the filtrates were washed by 200 μL of PBS for three times to remove the free components. Afterwards, the solution of protein complexes retained on the ultrafiltration membrane was transferred to a new tube. The bound ligand with specific binding to FKBP38 was separated by culturing with 60% ice methanol for 10 min. After repeating three times, the above filtrates were dried by nitrogen and reconstituted in 50 μL of 60% methanol, and subsequently analyzed using high-performance liquid chromatography−quadrupole-quadrupole-quadrupole−MS/MS (HPLC−QQQ−MS/MS)[14,15].

2.13. Thermal shift assay

The thermal shift assay was performed as previously described[16]. For the living cell temperature-dependent thermal shift assay, HL7702 hepatocytes were incubated with 20 μmol/L of HMF for 18 h, then the cells were heated at each temperature point from 37 to 60 °C for 3 min. The samples were centrifuged at 20,000 × *g* for 10 min at 4 °C to separate the supernatants and pellets, and then separated on a 10% SDS-PAGE for immunoblotting analysis of FKBP38.

2.14. Metabolic analysis

Total cholesterol (TC), TG levels, low-density lipoprotein cholesterol (LDL-c), and high-density lipoprotein cholesterol (HDL-c) levels in mice serum, homogenized liver tissues, and homogenized mice feces were measured using TG, TC, LDL-c, and HDL-c kits (Applygen, China) according to the manufacturer's instructions. Alanine aminotransferase (ALT) and aspartate aminotransferase (AST) levels in mice serum were measured using ALT and AST kits (Jiancheng, China).

An insulin tolerance test (ITT) was performed after a 6-h fast. Blood glucose level was measured before intraperitoneal injection of insulin (0.75 U/kg) and then 30, 60, 90, 120, or 150 min after injection. Glucose tolerance testing (GTT) was performed after overnight fasting. Blood glucose levels were measured before intraperitoneal injection of glucose (2 g/kg body weight) and then 15, 30, 60, 90, and 120 min after injection. Area under the curve (AUC) was calculated to quantify the oral glucose tolerance test (OGTT) and ITT results.

2.15. Liver-specific Fkbp38 knockdown

Six-week-old male C57BL/6J mice were injected with one single dose of 80 μL of adeno-associated virus 8 (AAV8)-*Fkbp38* short hairpin RNA (shRNA) virus suspension (virus titer>10^{12}) or AAV8-negative control shRNA (AAV8-NC shRNA) through the caudal vein. Livers were collected 35 days after infection, and qRT-PCR and immunoblotting was used to measure knockdown efficiency. The shRNA oligo sequences are as follows: NC shRNA: 5′-UUCUCCGAACGUGUCACGUTT-3′, 3′-ACGUGACACGUUCGGAGAATT-5′; *Fkbp38* shRNA: 5′-GCTCTCAAAGCTGGTAAAGAA-3′, 3′-TTCTTTACCAGCTTTGAGAGC-5′.

2.16. Histological analysis of liver and adipose

Livers and epididymal adipose tissues (WAT) were fixed in 4% PFA and embedded in paraffin wax. Paraffin sections (5 μm) were stained with haematoxylin and eosin (H&E). Sections were

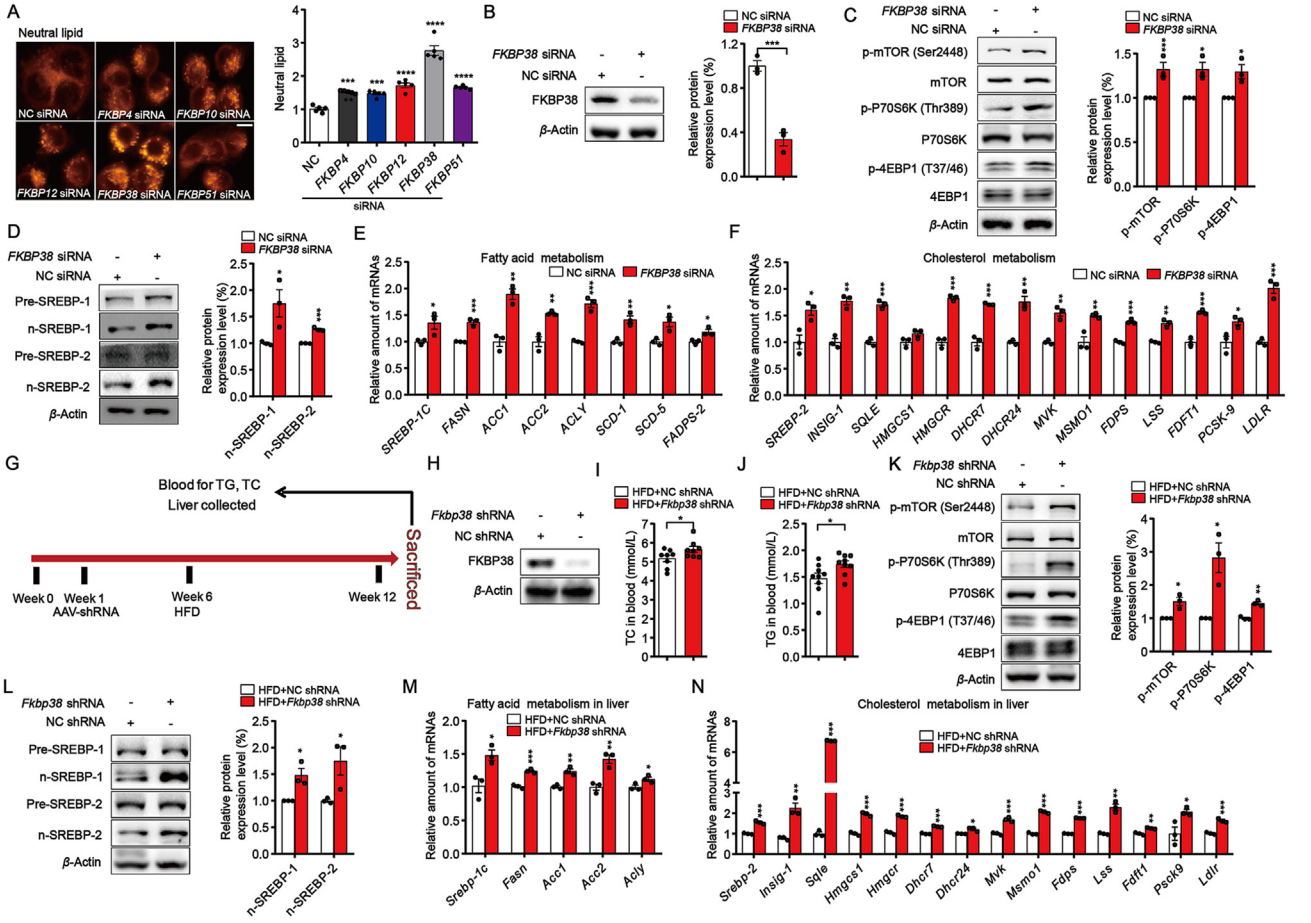

Figure 1 FKBP38 modulates mTOR/P70S6K/SREBP pathway and lipid level. (A) Measurement (left panel) and the quantification (right panel) of lipid content by Nile red fluorescence in HL7702 cells 18 h after transfection either with negative control (NC) siRNA or FKBPs siRNA, $n = 6$. Scale bar, 50 μm. (B) Western blot (left panel) and quantification (right panel) of FKBP38 protein level in HL7702 cells 18 h after treatment with NC siRNA or *FKBP38* siRNA, $n = 3$. (C, D) Western blot (left panel) and quantification (right panel) of the phophorylation of mTOR signaling (C) and nuclear SREBP protein expression (D) in HL7702 cells 18 h after treatment with NC siRNA or *FKBP38* siRNA, β-actin levels served as loading control, $n = 3$. (E, F) The expression of *SREBP-1C* target genes (E) and *SREBP-2* target genes (F) in HL7702 cells 18 h after treatment with NC siRNA or *FKBP38* siRNA, $n = 3$. (G) The schematic of experimental design. (H) FKBP38 protein in liver tissue of HFD-fed mice treated with *Fkbp38* shRNA or NC shRNA, $n = 3$. (I, J) Total cholesterol (TC, I) and triglyceride (TG, J) contents in serum of HFD-fed mice with *Fkbp38* shRNA or NC shRNA, $n = 8–9$. (K, L) Western blot (left panel) and quantification (right panel) of the phophorylation of mTOR signaling (K) and nuclear SREBP protein expression (L) in liver tissue of HFD-fed mice treated with *Fkbp38* shRNA or NC shRNA, β-actin levels were used as control for normalization, $n = 3$. (M, N) Relative mRNA abundance of *Srebp-1c* target genes (M) and *Srebp-2* target genes (N) in liver tissue of HFD-fed mice treated with *Fkbp3*8 shRNA or NC shRNA, $n = 3$. Data are represented as mean ± SEM. Comparisons between two groups were analyzed by using a two-tailed Student's *t* test. $^{*}P < 0.05$, $^{**}P < 0.01$, $^{***}P < 0.001$, $^{****}P < 0.0001$.

examined under digital pathological section scanner (NanoZoomer 2.0 RS, Hamamatsu, Japan).

2.17. Statistical analysis

All data are expressed as mean ± standard error of the mean (SEM). Comparisons between two groups were analyzed by using a two-tailed Student's *t* test, and those among three or more groups by using one-way analysis of variance (ANOVA) followed by Dunnett's *post hoc* tests. Differences were considered significant at $P < 0.05$. Statistical significance analyses were performed using GraphPad Prism version 7.0 (GraphPad Software, San Diego, CA, USA).

3. Results

3.1. FKBP38 suppresses mTOR/P70S6K/SREBP signaling and lipid level

FKBPs regulate inflammation and adaptive immune responses through multiple mechanisms including inhibition of mTOR[10]. Given that mTOR plays an important role in lipid biosynthesis[17,18], we reasoned that FKBPs are potential therapeutic targets for treatment of hyperlipidemia. To investigate whether FKBPs regulates lipid metabolism, we used specific siRNAs to knockdown five FKBPs (*FKBP4*, *FKBP10*, *FKBP12*, *FKBP38*, and *FKBP51*) transcripts, respectively (Supporting Information Fig. S1A) in HL7702 hepatocytes. Among these FKBPs,

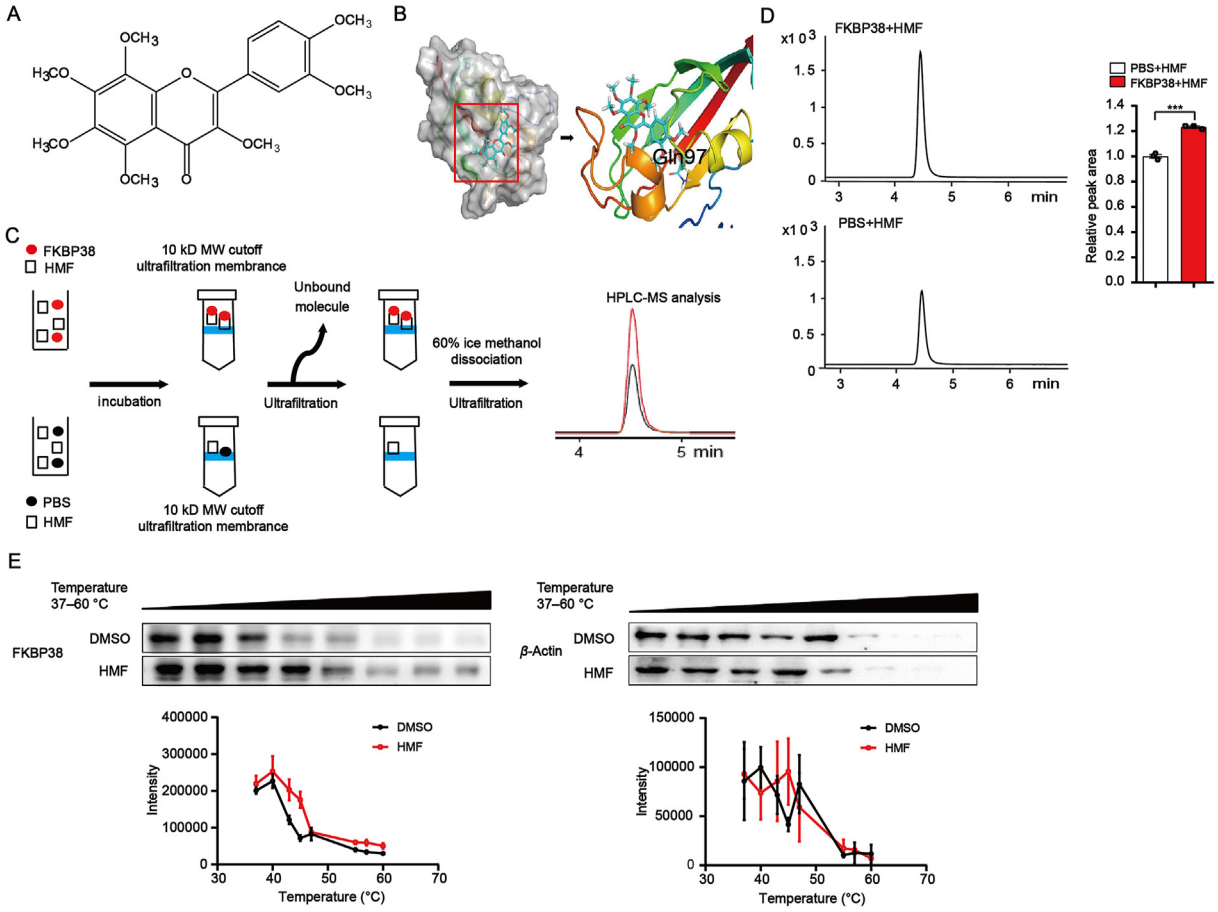

Figure 2 HMF targets FKBP38 to decrease cellular lipid level. (A) The structure of HMF. (B) Molecular docking analysis of the interaction between HMF and FKBP38, (PDB: 2F2D). (C) The schematic diagram of ultrafiltration-LC/MS analysis assays. (D) The affinity between HMF and FKBP38 was tested by HPLC−QQQ−MS/MS, $n = 3$. (E) HMF treatment (20 μmol/L) increases the thermal stability of FKBP38 in cells as measured by the temperature-dependent cellular thermal shift assay, $n = 3$. Data are represented as mean ± SEM. Comparisons between two groups were analyzed by using a two-tailed Student's *t* test. ***$P < 0.001$ *vs.* the PBS + HMF group.

knockdown of *FKBP38* markedly elevated the level of lipid content as measured by Nile red fluorescence and BODIPY (493/503) staining (Fig. 1A; Supporting Information Fig. S1B and S1C), indicating that FKBP38 is a negative regulator for lipid biosynthesis. We next examined whether FKBP38 regulates lipogenesis through mTOR activity. Consistent with the fact that FKBP38 bounds to mTOR and suppresses mTOR activity[19], knockdown of *FKBP38* significantly increased the phosphorylation of mTOR as well as its downstream targets P70S6K and 4EBP1 (Fig. 1B and C). Since many lines of evidence suggest that mTOR-mediated control of lipogenesis through SREBPs in hepatocytes[20], we further assessed whether SREBPs are involved in FKBP38-mediated lipogenesis. As shown in Fig. 1D, knockdown of *FKBP38* conspicuously up-regulated the protein levels of n-SREBP-1 and n-SREBP-2, but did not activate pre-SREBP-1 and pre-SREBP-2. We also observed a significant increase of the mRNA levels of *SREBP-1C*, *SREBP-2*, and their target genes involved in lipid metabolism, such as *FASN*, *ACC-1*, *SCD-1*, *HMGCR*, and *LDLR*, by *FKBP38* deletion (Fig. 1E and F). In line with the knockdown studies, overexpression of *FKBP38* in HL7702 cells (Supporting Information Fig. S2A) significantly reduced the lipid level (Supporting Information Fig. S2B), dephosphorylated phosphorylated mTOR, phosphorylated P70S6K, and phosphorylated 4EBP1 (Supporting Information Fig. S2C), down-regulated the protein levels of n-SREBP-1 and n-SREBP-2 (Supporting Information Fig. S2D), as well as the mRNA levels of *SREBP-1C*, *SREBP-2*, and their target genes (Supporting Information Fig. S2E and S2F). These observations suggested that FKBP38 reduces hepatic lipid content through mTOR−SREBPs signaling.

To further examine the function of FKBP38 *in vivo*, we deleted *Fkbp38* in mice livers by administration of AAV8-shRNA followed by a challenge of HFD for 6 weeks to induce hyperlipidemia (Fig. 1G and H). Liver-specific knockdown of *Fkbp38* in HFD-fed mice led to augment in blood and liver TC and TG levels (Fig. 1I and J; Supporting Information Fig. S1D and S1E). Similarly to the *in vitro* observations, *Fkbp38* inactivation up-regulated the phosphorylation of mTOR, P70S6K, and 4EBP1 (Fig. 1K), increased the protein levels of n-SREBP-1 and n-SREBP-2 (Fig. 1L), as well as the mRNA levels of *Srebp1-c*, *Srebp-2*, and their target genes in liver tissues (Fig. 1M and N). Taken together, we identified FKBP38 as a key regulator for FFA and cholesterol biosynthesis through the mTOR/P70S6K/SREBPs pathway.

3.2. *HMF targets FKBP38 to decrease cellular lipid level*

As FKBP38 is an attractive target for hyperlipidemia treatment, we sought to identify specific small molecules targeting FKBP38 by

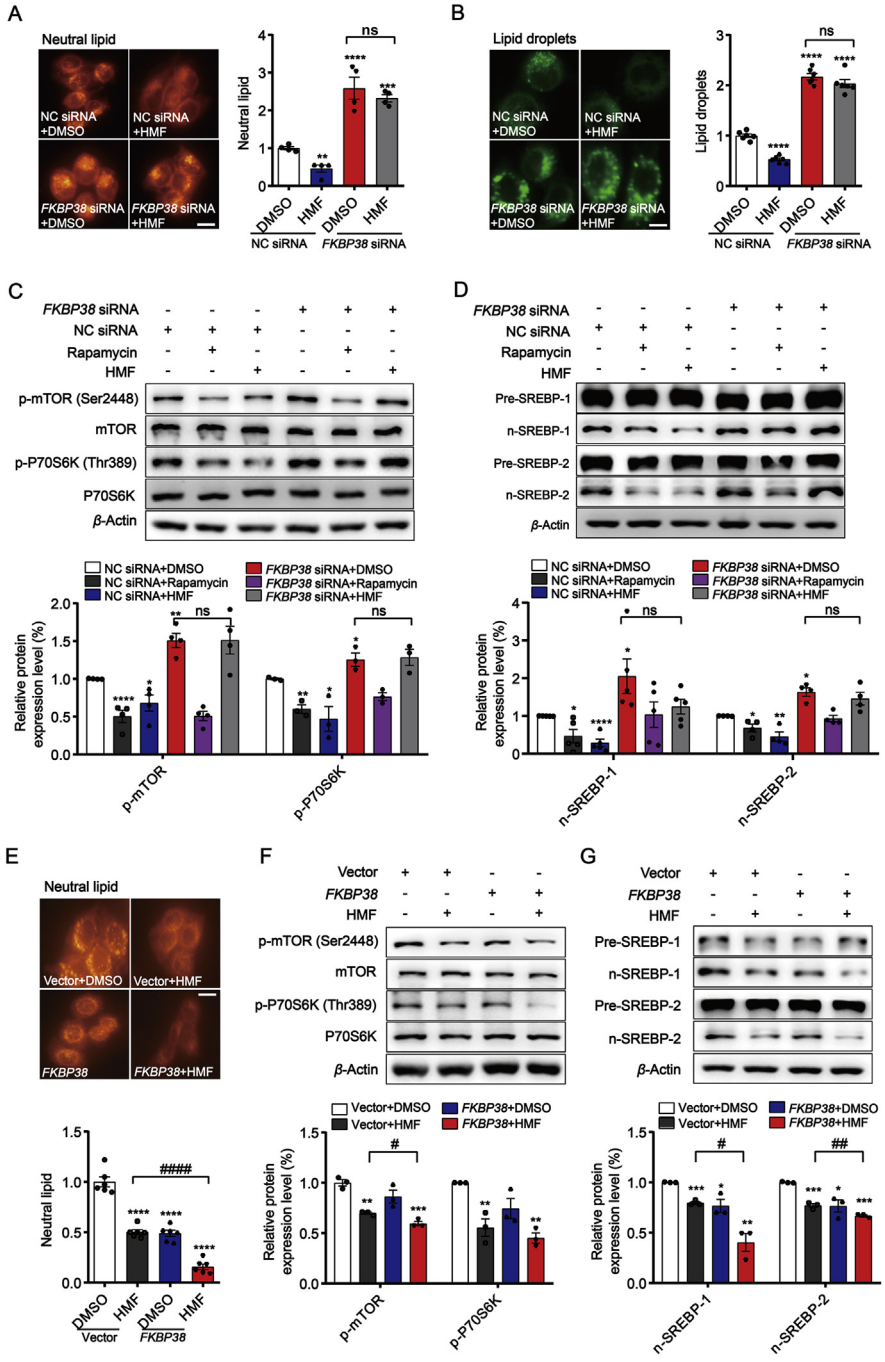

Figure 3 Inhibition of mTOR/P70S6K/SREBPs pathway by HMF is dependent on FKBP38. (A) Measurement (left panel) and the quantification (right panel) of lipid content by Nile red fluorescence in HL7702 cells incubated with LD medium in the presence of DMSO or HMF (20 μmol/L) 18 h after transfection either with NC siRNA or *FKBP38* siRNA, $n = 4$. Scale bar, 50 μm. (B) Measurement (left panel) and the quantification (right panel) of lipid droplets by BODIPY (493/503) Staining in HL7702 cells incubated with LD medium in the presence of DMSO or HMF (20 μmol/L) 18 h after transfection either with NC siRNA or *FKBP38* siRNA, $n = 6$. Scale bar, 50 μm. (C, D) Western blot (top panel) and quantification (bottom panel) of the protein expression of phophorylation of mTOR signaling (C) and nuclear SREBP protein expression (D) in HL7702 cells incubated with LD medium in the presence of DMSO or HMF (20 μmol/L) 18 h after treatment with NC siRNA or *FKBP38* siRNA, β-actin levels served as loading control, $n = 3-5$. (E) Measurement (top panel) and the quantification (bottom panel) of lipid content by Nile red fluorescence in HL7702 cells incubated with LD medium in the presence of DMSO or HMF (20 μmol/L) 18 h after transfection either with empty vector or FKBP38-overexpression plasmids, $n = 6$. Scale bar, 50 μm. (F, G) Western blot (top panel) and quantification (bottom panel) of the protein expression of phophorylation of mTOR signaling (F) and nuclear SREBP protein expression (G) in HL7702 cells incubated with LD medium in the presence of DMSO or HMF (20 μmol/L) 18 h after treatment with empty vector or FKBP38-overexpression plasmids, β-actin levels served as loading control, $n = 3$. Data are represented as mean ± SEM. Comparisons between two groups were analyzed by using a two-tailed Student's *t* test, and those among three or more groups by using one-way ANOVA followed by Dunnett's *post hoc* tests. $^{*}P < 0.05$, $^{**}P < 0.01$, $^{***}P < 0.001$, $^{****}P < 0.0001$ *vs.* the NC + DMSO group or Vector group; $^{\#}P < 0.05$, $^{\#\#}P < 0.01$, $^{\#\#\#\#}P < 0.0001$ *vs.* the Vector + HMF group. ns, no significance.

docking approach. From a small molecule pool containing 504 natural compounds (Supporting Information Table S2), HMF (Fig. 2A), a citrus flavonoid, was found to fit into the protein pocket of FKBP38 with the lowest binding energy of −6.71 kcal/mol. HMF had a hydrogen bond at Gln97 with FKBP38, which maintained the binding stability (Fig. 2B), but it bound poorly with other FKBPs (Supporting Information Table S3). To further assess whether HMF bounds to FKBP38, we performed the ultrafiltration-LC/MS analysis and observed the binding of HMF and FKBP38, as reflected by the increase of MS response (Fig. 2C and D). The temperature-dependent cellular thermal shift assays demonstrated that HMF affected the thermal stability of FKBP38 (Fig. 2E), supporting that there is a direct interaction between FKBP38 and HMF. Collectively, these results indicate that FKBP38 is a direct target of HMF.

We next examined whether HMF can affect lipid metabolism. Similar with the effect of LOV, a well-known treatment of hyperlipidemia, HMF reduced lipid content in HL7702 hepatocytes as measured by Nile red fluorescence (Supporting Information Fig. S3A). In addition, HMF treatment reduced lipid droplets as measured by BODIPY (493/503) staining (Supporting Information Fig. S3B). Without discernible toxicity (Supporting Information Fig. S3C), HMF treatment also decreased the phosphorylation level of mTOR and P70S6K (Supporting Information Fig. S3D), protein expression of n-SREBP-1 and n-SREBP-2 (Supporting Information Fig. S3E), SRE-luciferase activity of SREBPs (Supporting Information Fig. S3F and

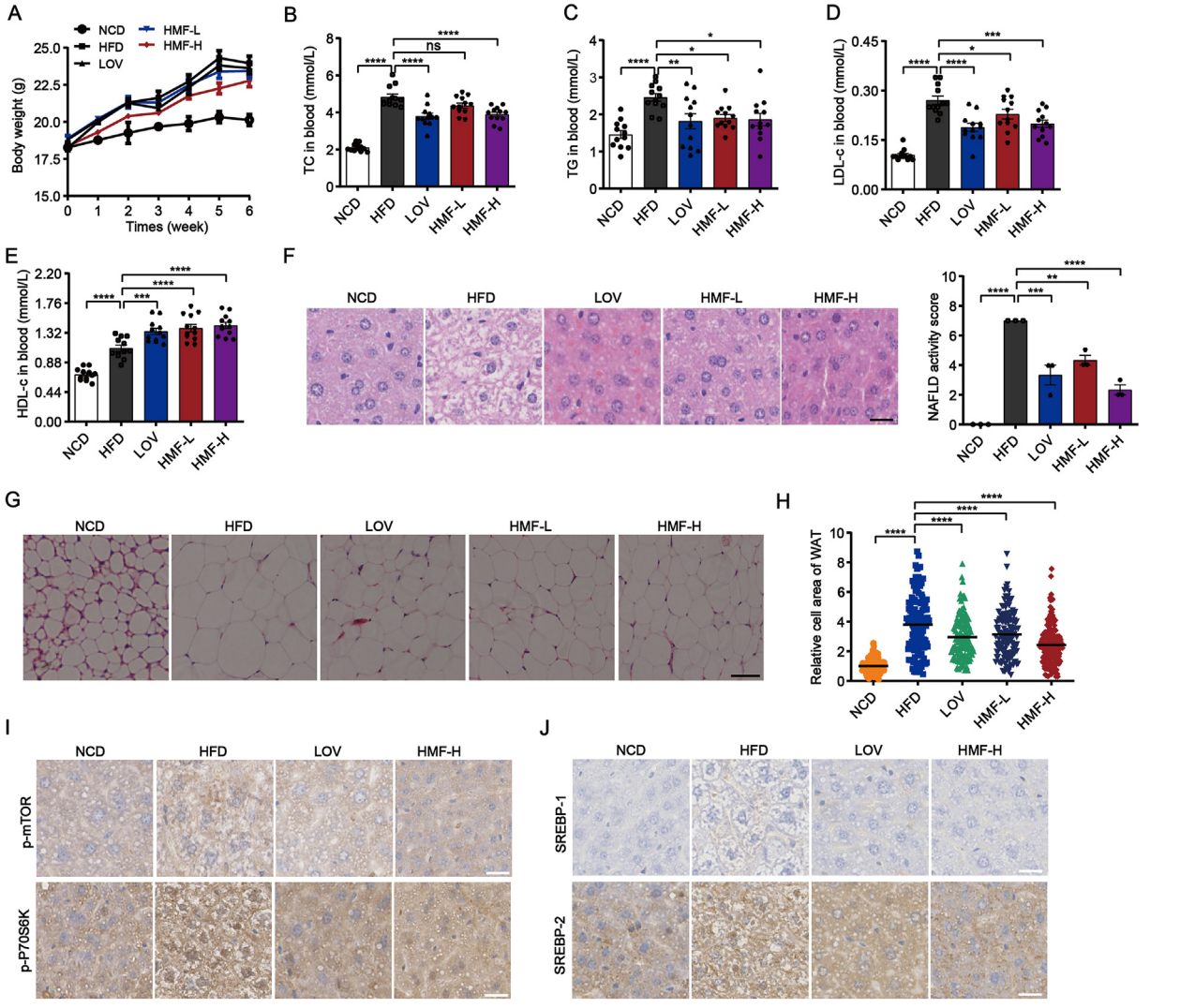

Figure 4 HMF potently ameliorates diet-induced obesity and hyperlipidemia. Vehicle, LOV (30 mg/kg/day), or HMF (25 or 50 mg/kg/day) was administrated to HFD mice by gastric irrigation once daily for 6 weeks. The mice were finally sacrificed and subjected to various analyses as indicated below. (A) Time-course of body weight, $n = 11-12$/group. (B–E) Measurement of TC (B), TG (C), low-density lipoprotein cholesterol (LDL-c, D), and high-density lipoprotein cholesterol (HDL-c, E) in serum, $n = 11-12$/group. (F) Liver staining with haematoxylin and eosin (H&E) (left panel) and the NAFLD activity score (right panel), $n = 3$. Scale bar, 50 μm. (G) White adipose tissue staining with H&E, $n = 3$. Scale bar, 50 μm. (H) Quantification of relative area epididymal adipose tissues (WAT), $n = 3$. (I, J) Immunohistochemistry staining analysis of phosphorylated mTOR, phosphorylated P70S6K (I), SREBP-1 and SREBP-2 (J) in liver tissues, $n = 3$. Scale bar, 50 μm. NCD, normal chow diet; HFD, high-fat diet; LOV, lovastatin (30 mg/kg/day); HMF-L, HMF (25 mg/kg/day); HMF-H, HMF (50 mg/kg/day). Data are represented as mean ± SEM. Comparisons between two groups were analyzed by using a two-tailed Student's *t* test, and those among three or more groups by using one-way ANOVA followed by Dunnett's *post hoc* tests. $^{*}P < 0.05$, $^{**}P < 0.01$, $^{***}P < 0.001$, $^{****}P < 0.0001$ *vs.* the HFD group.

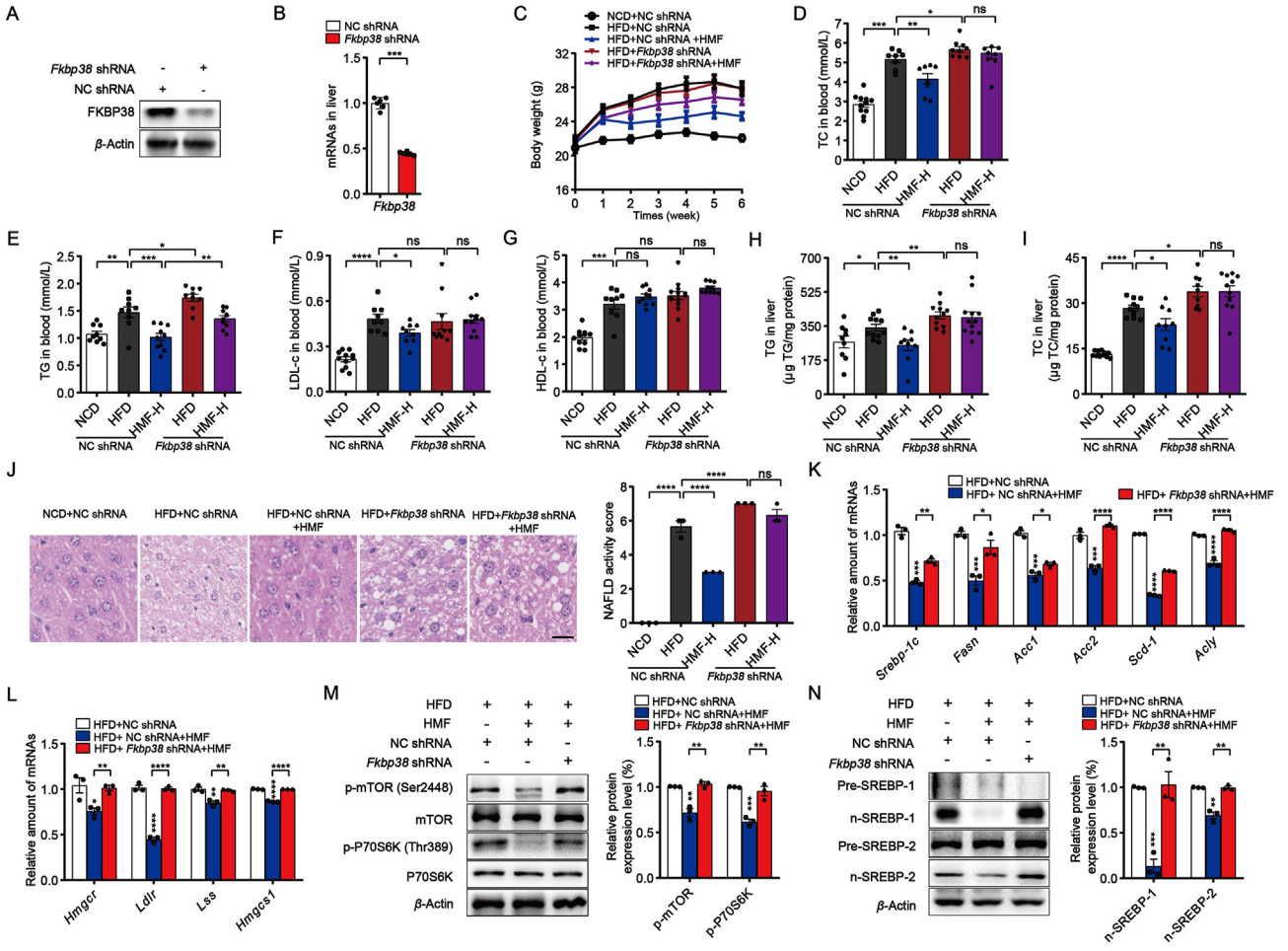

Figure 5 *Fkbp38* knockdown relieves the hypolipidemic effect of HMF in HFD mice. Male 6-week-old C57BL/6J mice were injected with NC shRNA or *Fkbp38* shRNA adenoviruses. Five weeks after injection, vehicle or HMF (50 mg/kg/day) was administrated to NCD-fed, HFD-fed mice by gastric irrigation once daily for 6 weeks. The mice were finally sacrificed and subjected to various analyses as indicated below. (A, B) *Fkbp38* mRNAs (A) and FKBP38 protein expression (B) in liver tissues of mice treated with *Fkbp38* shRNA or NC shRNA, $n = 3$. (C) Time-course of body weight, $n = 9-12$/group. (D–G) Serum TC (D), TG (E), LDL-c (F), and HDL-c (G), $n = 9-11$/group. (H, I) Total triglycerides (H) and total cholesterol (I) in liver, $n = 9-11$/group. (J) Liver staining with H&E (left panel) and the NAFLD activity score (right panel), $n = 3$. Scale bar, 50 μm. (K, L) Relative expression level of genes in FFA metabolism and cholesterol biosynthesis in livers, $n = 3$. (M, N) Western blot (left panel) and quantification (right panel) of the protein expression of phophorylation of mTOR signaling (M) and nuclear SREBP protein expression (N) in livers, β-actin levels served as loading control, $n = 3$. Data are represented as mean ± SEM. Comparisons between two groups were analyzed by using a two-tailed Student's *t* test, and those among three or more groups by using one-way ANOVA followed by Dunnett's *post hoc* tests. $^*P < 0.05$, $^{**}P < 0.01$, $^{***}P < 0.001$, $^{****}P < 0.0001$ *vs.* the HFD + NC shRNA group.

S3G), and mRNA levels of *SREBP-1C*, *SREBP-2*, as well as their target genes in a dose-dependent manner (Supporting Information Fig. S3H and S3I). MHY1485, a potent mTOR activator, restored the activity of mTOR and P70S6K activity, expression of mature *SREBP-1*, *SREBP-2*, and their target genes in HMF-treated cells (Supporting Information Fig. S4A–S4C). Since the activity of mTOR is also regulated by AKT, AMPKα, and GSK-3β, we assessed whether these signal pathways are affected by HMF. However, HMF showed no discernible effect on the phosphorylation of AKT, AMPKα, and GSK-3β (Supporting Information Fig. S4D). Collectively, these data indicate that HMF may function as a FKBP38 activator to inhibit mTOR activity and regulate lipid synthesis.

To further investigate whether HMF–FKBP38 interaction is required for HMF-mediated reduce of lipogenesis, we knocked down *FKBP38* in HMF-treated cells. As expected, *FKBP38* inactivation diminished the reduction of lipid content by HMF (Fig. 3A and B), reversed the HMF-induced dephosphorylation of mTOR and P70S6K (Fig. 3C), as well as the reduction of the expression of n-SREBP-1 and n-SREBP-2 (Fig. 3D). In contrast, *FKBP38* overexpression augmented HMF-mediated reduction of lipid production (Fig. 3E; Supporting Information Fig. S4E), dephosphorylation of mTOR and P70S6K (Fig. 3F), and reduction of n-SREBP-1 and n-SREBP-2 (Fig. 3G). Taken together, these data indicate that FKBP38 activation is required for HMF-mediated reduction of lipogenesis.

3.3. *HMF potently ameliorates diet-induced obesity and hyperlipidemia and improves insulin resistance in mice*

We next investigate the effect of HMF on hyperlipidemia *in vivo*. We fed C57BL/6J mice with HFD for 6 weeks and supplemented HMF or saline in the diet daily. HFD feeding led to significant

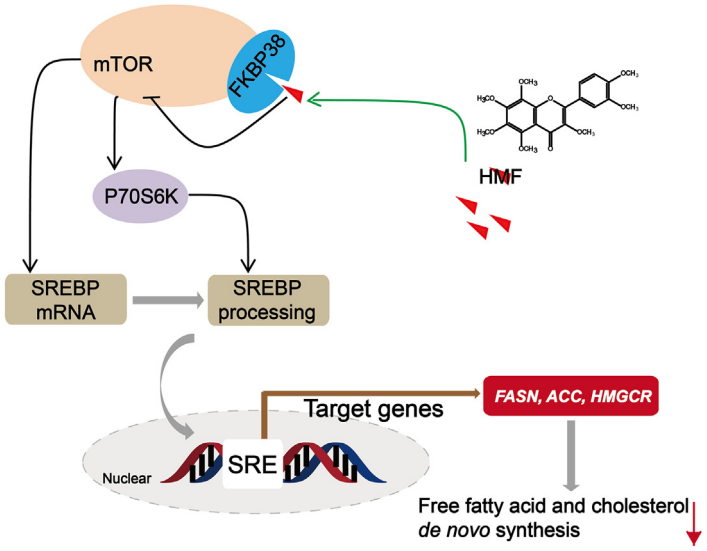

Figure 6 Proposed mechanism of HMF-mediated hypolipidemic effect. HMF targets FKBP38 to suppress mTOR/P70S6K/SREBPs pathway, which mediate the *de novo* synthesis of free fatty acid and cholesterol.

increases in body weight, serum TG, TC, and LDL-c compared with control, while HMF significantly reduced these hyperlipidemic traits in a dose-dependent manner (Fig. 4A−D). Also, the HDL-c was markedly increased in HMF-treated mice (Fig. 4E). No significant difference in food intake, fecal cholesterol, and TG was observed among HMF or saline treated HFD mice (Supporting Information Fig. S5A−S5C), indicating HMF-ameliorated hyperlipidemia is not due to the change of food consumption and lipid excretion. HMF treatment also lowered lipid accumulation in liver, reduced the cell size of white adipocyte tissue (Fig. 4F−H), and exhibited protective effects against the HFD-induced liver damage as supported by significantly lower plasma ALT and AST levels (Supporting Information Fig. S5D and E). Additionally, HMF-treated mice markedly restore glucose intolerance (Supporting Information Fig. S5F) and insulin resistance (Supporting Information Fig. S5G−S5J) induced by HFD. Consistent with *in vitro* results, immunohistochemistry analysis demonstrated that HMF inhibited the phosphorylation of mTOR and P70S6K (Fig. 4I), decreased the expression of SREBP-1 and SREBP-2 compared to HFD-fed group (Fig. 4J). For genes in free fatty acid (FFA) metabolism and cholesterol biosynthesis, HMF significantly decreased the mRNA levels of *Fasn*, *Acc1*, *Scd-1*, *Hmgcr*, *Ldlr*, *Tnf-α*, and *Il-1β* in the livers of HMF-treated mice (Supporting Information Fig. S5K). These results indicate that HMF exhibits robust efficacy against hyperlipidemia in HFD-fed mice.

3.4. Fkbp38 knockdown relieves the hypolipidemic effect of HMF in HFD mice

To assess whether HMF activates FKBP38 to relieve hyperlipidemia and improve insulin resistance, we knocked down *Fkbp38* in mice liver by AAV8-*Fkbp3*8 shRNA (Fig. 5A and B) in HFD-fed mice. We observed negligible toxicity and food intake in HMF or AAV8-*Fkbp3*8 shRNA treated HFD mice (Supporting Information Fig. S6A). Liver-specific knockdown of *Fkbp38* abolished not only HMF-induced reduction of body-weight gain, lipid accumulation in blood and liver, liver damage (Fig. 5C−J; Supporting Information Fig. S6B and S6C), but also HMF-induced amelioration of blood glucose, glucose tolerance, and insulin resistance (Supporting Information Fig. S6D−S6H), suggesting that FKBP38 is essential for the hypolipidemic effects of HMF in HFD-fed mice. Liver-specific knockdown of *Fkbp38* also blunted the decreased phosphorylation of mTOR and P70S6K as well as the inhibited expression of SREBPs and their target genes by HMF treatment (Fig. 5K−N). Together, these results indicate that the hypolipidemic effects of HMF are mostly ascribed to targeting FKBP38 to suppress the mTOR/P70S6K/SREBPs pathway.

4. Discussion

A large body of evidence indicates that mTOR signaling regulates specific transcription factors (*e.g.*, SREBPs) and promotes lipogenesis[21−25]. mTORC1 can exert regulation on SREBP-1 activity *via* activation of S6 kinase 1 (S6K1)[26]. However, many researchers report that treatment of rodents or humans with rapamycin leads to hyperlipidemia[4]. From a clinical perspective, the development of mTOR-specific inhibitors should reduce the side effects associated with rapamycin. Here, we came up an alternative strategy to activate mTOR endogenous inhibitors and decrease hyperlipidemia. FKBP38 is a member of FKBPs, which binds and inhibits mTORC1 function[10]. However, its role in lipid metabolism remains unclear. In this study, we demonstrated that FKBP38 was actively involved in cholesterol, FA, and triglyceride biosynthesis by restraining mTOR/P70S6K pathway and SREBPs activity *in vitro* and *in vivo*. These results laid a solid foundation to identify FKBP38 as a potential target for hyperlipidemia treatment.

Although natural compounds are considered as an indispensable source of drugs and drug leads, it has proven difficult to identify their target proteins and elucidate the mechanism. Here, we reported a systematic strategy for screening of FKBP38-targeted small molecules employing docking approach, ultrafiltration-LC/MS analysis and temperature-dependent cellular

thermal shift assays. We identified HMF, a polymethoxyflavone isolated from citrus peel, can potently bind to FKBP38. FKBP38 inactivation and overexpression *in vitro* and AAV8-*Fkbp38* shRNA *in vivo* experiments confirmed that HMF targeted FKBP38 to produce hypolipidemic effects. Together, our study illustrates how integration of computational screening and functional data can identify mechanisms by which natural products regulate biological activities.

Recently, Feng et al.[27] reported that HMF prevented obesity in high-fat diet-induced rats by regulation of the expression of lipid metabolism-related and inflammatory response related genes. In this work, we found that HMF can bind and activate FKBP38 to inhibit phosphorylation of mTOR and P70S6K and SREBP activity, down-regulate the genes associated with cholesterol and FFA biosynthesis, and decrease the content of cellular lipids. We further confirmed that FKBP38 is required for the hypolipidemic effect of HMF as evidenced by elevated lipid level after *Fkbp38* silencing. Statins, inhibitors of HMGCR, are the most widely prescribed drugs to treat hypercholesterolemia *via* blocking cholesterol biosynthesis. However, statin activates SREBPs and raises cholesterol and fatty acid biosynthetic enzymes in liver, which lead to adverse effects[28,29]. Notably, HMF ameliorated obesity, insulin resistance, fatty accumulation in liver and hyperlipemia without apparent side effects, indicating HMF is a prospective and safe drug target to lower lipid levels.

HMF has been reported to have wide biological activities including anti-tumor, anti-inflammation, and neuroprotective properties[30−32]. From this study, we demonstrated that HMF can function as mTOR inhibitor, which may expand its clinical potential in transplantation and autoimmune disease without hyperlipidemic side effects.

5. Conclusions

Our *in vivo* and *in vitro* results reveal that FKBP38 plays a crucial role in regulating mTOR/P70S6K/SREBPs pathway as well as cholesterol, FFA, and triglyceride biosynthesis. Interestingly, we found that the small molecule HMF specifically targeted FKBP38 to suppress the mTOR/P70S6K/SREBPs pathway, thereby decrease lipid content *in vitro* and ameliorate hyperlipidemia in HFD-fed mice (Fig. 6). Our study sheds some light on the key role of FKBP38 in hyperlipidemia, and indicates that HMF may serve as a leading compound for the pharmacological control of metabolic diseases.

Acknowledgments

We greatly appreciate financial support from the National Natural Science Foundation of China (81922072 and 81973443), “Double First-Class” University project (CPU2018PZQ16 and CPU2018GF04, China), the Project of State Key Laboratory of Natural Medicines (SKLNMZZ202006, China), the Open Project of State Key Laboratory of Natural Medicines (SKLNMKF202010, China), and a Project Funded by the Priority Academic Program Development of Jiangsu Higher Education Institutions (China).

Author contributions

E-Hu Liu, Ping Li, Chun Zeng, Zhi-shen Xie, and Ping-ting Xiao designed the study protocol and supervised all parts of the project. Ping-ting Xiao, Zhi-shen Xie, Yu-jia Kuang, and Shi-yu Liu conducted animal experiments and the molecular biology experiments. Ping-ting Xiao and Zhi-shen Xie drafted the first versions. E-Hu Liu, Ping Li, and Chun Zeng contributed to text revision and discussion.

Conflicts of interest

The authors have no conflicts of interest to declare.

Appendix A. Supporting information

Supporting data to this article can be found online at https://doi.org/10.1016/j.apsb.2021.03.031.

References

1. Tang JJ, Li JD, Qi W, Qiu WW, Li PS, Li BL, et al. Inhibition of SREBP by a small molecule, betulin, improves hyperlipidemia and insulin resistance and reduces atherosclerotic plaques. *Cell Metab* 2011;**13**:44−56.
2. Shattat GF. A review article on hyperlipidemia: types, treatments and new drug targets. *Biomed Pharmacol J* 2015;**7**:399−409.
3. Goldstein JL, DeBose-Boyd RA, Brown MS. Protein sensors for membrane sterols. *Cell* 2006;**124**:35−46.
4. Peterson TR, Sengupta SS, Harris TE, Carmack AE, Kang SA, Balderas E, et al. mTOR complex 1 regulates lipin 1 localization to control the SREBP pathway. *Cell* 2011;**146**:408−20.
5. González A, Hall MN, Lin SC, Hardie DG. AMPK and TOR: the yin and yang of cellular nutrient sensing and growth control. *Cell Metab* 2020;**31**:472−92.
6. Ardestani A, Lupse B, Kido Y, Leibowitz G, Maedler K. mTORC1 signaling: a double-edged sword in diabetic β cells. *Cell Metab* 2018;**27**:314−31.
7. Lamming DW, Sabatini DM. A central role for mTOR in lipid homeostasis. *Cell Metab* 2013;**18**:465−9.
8. Houde VP, Brûlé S, Festuccia WT, Blanchard PG, Bellmann K, Deshaies Y, et al. Chronic rapamycin treatment causes glucose intolerance and hyperlipidemia by upregulating hepatic gluconeogenesis and impairing lipid deposition in adipose tissue. *Diabetes* 2011;**59**:1138−48.
9. Bai XC, Ma DZ, Liu AL, Shen XY, Wang QJ, Liu YJ, et al. Rheb activates mTOR by antagonizing its endogenous inhibitor, FKBP38. *Science* 2007;**318**:977−80.
10. Jiang Y, Tong M. FK506-binding proteins and their diverse functions. *Curr Mol Pharmacol* 2016;**9**:48−65.
11. Zeng SL, Li SZ, Xiao PT, Cai YY, Chu C, Chen BZ, et al. Citrus polymethoxyflavones attenuate metabolic syndrome by regulating gut microbiome and amino acid metabolism. *Sci Adv* 2020;**6**:eaax6208.
12. Gao M, Su HF, Lin YH, Ling X, Li SW, Qin AJ, et al. Photoactivatable aggregation-induced emission probes for lipid droplets-specific live cell imaging. *Chem Sci* 2017;(8):1763−8.
13. Jiang SY, Li H, Tang JJ, Wang J, Luo J, Liu B, et al. Discovery of a potent HMG-CoA reductase degrader that eliminates statin-induced reductase accumulation and lowers cholesterol. *Nat Commun* 2018;**9**:5138.
14. Qin SS, Ren YR, Fu X, Shen J, Chen X, Wang Q, et al. Multiple ligand detection and affinity measurement by ultrafiltration and mass spectrometry analysis applied to fragment mixture screening. *Anal Chim Acta* 2015;**886**:98−106.
15. Chen GL, Fan MX, Wu JL, Li N, Guo MQ. Antioxidant and anti-inflammatory properties of flavonoids from lotus plumule. *Food Chem* 2019;**277**:706−12.
16. Dai JY, Liang K, Zhao S, Jia WT, Liu Y, Wu HK, et al. Chemoproteomics reveals baicalin activates hepatic cpt1 to ameliorate diet-induced obesity and hepatic steatosis. *Proc Natl Acad Sci U S A* 2018;**115**:E5896−905.

17. Laplante M, Sabatini DM. An emerging role of mTOR in lipid biosynthesis. *Curr Bio* 2009;**19**:R1046−52.
18. Sengupta S, Peterson TR, Sabatini DM. Regulation of the mTOR complex 1 pathway by nutrients, growth factors, and stress. *Mol Cell* 2010;**40**:310−22.
19. Ma D, Bai X, Guo S, Jiang Y. The switch I region of Rheb is critical for its interaction with FKBP38. *J Biol Chem* 2008;**283**:25963−70.
20. Quinn 3rd WJ, Birnbaum MJ. Distinct mTORC1 pathways for transcription and cleavage of SREBP-1c. *Proc Natl Acad Sci U S A* 2012;**109**:15974−5.
21. Lewis CA, Griffiths B, Santos CR, Pende M, Schulze A. Regulation of the SREBP transcription factors by mTORC1. *Biochem Soc Trans* 2011;**39**:495−9.
22. Owen JL, Zhang YY, Bae SH, Farooqi MS, Liang GS, Hammer RE, et al. Insulin stimulation of SREBP-1c processing in transgenic rat hepatocytes requires p70 S6-kinase. *Proc Natl Acad Sci U S A* 2012;**109**:16184−9.
23. Wu XY, Romero D, Swiatek WI, Dorweiler I, Kikani CK, Sabic H, et al. PAS kinase drives lipogenesis through SREBP-1 maturation. *Cell Rep* 2014;**8**:242−55.
24. Yecies JL, Zhang HH, Menon S, Liu S, Yecies D, Lipovsky AI, et al. Akt stimulates hepatic SREBP1c and lipogenesis through parallel mTORC1-dependent and independent pathways. *Cell Metab* 2011;**14**:21−32.
25. Ben SI, Manning BD. mTORC1 signaling and the metabolic control of cell growth. *Curr Opin Cell Biol* 2017;**45**:72−82.
26. Mossmann D, Park S, Hall MN. mTOR signalling and cellular metabolism are mutual determinants in cancer. *Nat Rev Cancer* 2018;**18**:744−57.
27. Feng KL, Zhu XA, Chen T, Peng B, Lu MW, Zheng H, et al. Prevention of obesity and hyperlipidemia by heptamethoxyflavone in high-fat diet-induced rats. *J Agr Food Chem* 2019;**67**:2476−89.
28. Kita T, Brown MS, Goldstein JL. Feedback regulation of 3-hydroxy-3-methylglutaryl coenzyme a reductase in livers of mice treated with mevinolin, a competitive inhibitor of the reductase. *J Clin Invest* 1980;**66**:1094−100.
29. Singer II , Kawka DW, Kazazis DM, Alberts AW, Chen JS, Huff JW, et al. Hydroxymethylglutaryl-coenzyme A reductase-containing hepatocytes are distributed periportally in normal and mevinolintreated rat livers. *Proc Natl Acad Sci U S A* 1984;**81**:5556−60.
30. Iwase Y, Takemura Y, Ju-ichi M, Yano M, Ito C, Furukawa H, et al. Cancer chemopreventive activity of 3,5,6,7,8,3′,4′-heptamethoxyflavone from the peel of citrus plants. *Cancer Lett* 2001;**163**:7−9.
31. Manthey JA, Bendele P. Anti-inflammatory activity of an orange peel polymethoxylated flavone, 3′,4′,3,5,6,7,8-Heptamethoxyflavone, in the rat carrageenan/paw edema and mouse lipopolysaccharide-challenge assays. *J Agr Food Chem* 2008;**56**:9399−403.
32. Furukawa Y, Okuyama S, Amakura Y, Watanabe S, Fukata T, Nakajima M, et al. Isolation and characterization of activators of ERK/MAPK from citrus plants. *Int J Mol Sci* 2012;**13**:1832−45.